

# EXPERIMENTAL AND NUMERICAL ANALYSIS OF DAMAGED MASONRY BUILDING

Ivan Duvnjak <sup>(1)</sup>, Marina Frančić Smrkić <sup>(2)</sup>, Domagoj Damjanović <sup>(3)</sup>, Karla Grgić

<sup>(1)</sup> Assoc. Prof., University of Zagreb, Faculty of Civil Engineering, [ivan.duvnjak@grad.unizg.hr](mailto:ivan.duvnjak@grad.unizg.hr)

<sup>(2)</sup> Assist. Prof., University of Zagreb, Faculty of Civil Engineering, [marina.francic.smrkic@grad.unizg.hr](mailto:marina.francic.smrkic@grad.unizg.hr)

<sup>(3)</sup> Prof., University of Zagreb, Faculty of Civil Engineering, [domagoj.damjanovic@grad.unizg.hr](mailto:domagoj.damjanovic@grad.unizg.hr)

## Abstract

Recent seismic activity in Croatia has caused significant damage to a large number of old masonry buildings. Since the post-earthquake condition and mechanical properties are not known, on-site experimental testing is an important segment of the maintenance and repair of old masonry buildings. In this paper, the results of experimental determination of the mechanical properties and dynamic parameters on the damaged maisonette building of Sisak highschool are presented. In order to confirm and validate the experimental results, a numerical analysis of the building was performed. After making the initial FE model, the comparison between the natural frequencies obtained from the model and the experimental results revealed unsatisfactory outcomes. Therefore, the FE model was calibrated through a whole series of iterations: modification of the boundary conditions, modelling of partition walls, modelling of the damages and modification of the global stiffness of the structure. After a series of iterations, the global stiffness was significantly reduced by nearly 50% of the experimental results, ultimately leading to a satisfactory result. Apart from the reliability of the numerical model and the calibration of the numerical model analyzed here, by repeating the test after the future renovation (considering changes in building mass), the experimentally determined dynamic parameters of the structure can be used to verify the effects of the renovation of the building.

*Keywords: masonry, numerical modeling, experimental testing, dynamic properties, mechanical properties*

## 1 Introduction

Masonry buildings of traditional construction were mostly built at a time when there were no regulations for the construction of earthquake-resistant buildings. A large number of old masonry buildings have suffered significant damage from recent seismic activity. Due to the lack of knowledge about their condition and mechanical properties after the earthquake, experimental work is an important segment for future calculations of old masonry buildings [1]. The combination of experimental onsite testing and numerical analysis is often used in order to derive realistic information about the boundary conditions and the mechanical properties of the structure's constituent materials [2], [3]. These procedure typically consist in updating some parameters of the FE model in order to minimize the differences between numerical and experimentally obtained dynamic properties (natural frequencies and mode shapes) [4]. In this paper, the results of testing the mechanical properties and dynamic parameters on the damaged maisonette building of Sisak highschool are presented.

In order to validate the experimental results, a numerical analysis of the building was performed. The results of the natural frequencies of the numerical model compared to the experimentally obtained results were not satisfactory after first iteration of numerical model. Therefore, the model was updated through a whole series of iterations: modification of the boundary conditions, modelling of partition walls, modelling of the damage and modification of the global stiffness of the structure.

Highschool Sisak was built in 1935. The building has four floors: basement, ground floor and two floors, Figure 1. In the central part of the building there is a three-legged staircase with a landing. The foundations are constructed as a reinforced concrete slab. The load-bearing structure of the building consists of walls made of solid bricks, floor slabs and finely ribbed floor slabs made of reinforced concrete. At the entrance of the building on the first and second floors, there is a load-bearing part of the structure that rests on stone columns arranged in two rows.

## 2 Experimental analysis

During the investigation work, a visual inspection of the building was carried out and damage was observed on the load-bearing walls and partitions of the ground floor and the first floor. Some characteristic damage can be seen in Figure 2.



Figure 1. Sisak highschool building



Figure 2. Typical damage on the load-bearing wall

### 2.1 Experimental research of mechanical properties

Within the experimental investigation on highschool in Sisak, the following tests were conducted: *in situ* masonry shear strength, determination of existing compressive stress in masonry using *flat jacks*, determination of elasticity modulus.

Masonry shear strength testing is conducted using a small hydraulic jack by which a minimum damage is induced, Figure 3. After removing the plaster, a longitudinally oriented brick is selected. Before the test, head joint must be removed on one side of the brick and on the other side there should be enough space to install the hydraulic jack. The test involves determining shear strength  $f_V$  with the contribution of normal compressive stress  $\sigma_0$ . This is why it is important to accurately determine the test position, which enables the calculation of vertical load and the corresponding stress  $\sigma_0$ . Testing was performed on 15 measurement points, 5 on each floor. The mean value of the results on each floor are showed in Table 1.

Table 1. The results of shear strength  $f_V$  with the contribution of compressive stress

Position	Shear strength $f_V$ with standard deviation (MPa)
Ground floor	0,817 ± 0,149
First floor	0,652 ± 0,187
Second floor	0,515 ± 0,048
<b>Average value</b>	<b>0,661 ± 0,180</b>

The determination of the existing compressive stress in the masonry is conducted using single *flat jacks*, Figure 4, [5]. The compressive stress in the masonry is partially relieved by removing the mortar from the bed joint. The stress is then compensated by inserting the flat jack into the opening until the initial state of stress and strain is established, which is controlled by measuring the displacement perpendicular to the opening. It should be noted that the stress obtained in this test is an average value of the stress in the part of the wall near the opening, i.e. it can be assumed that the stress is representative for the entire wall only if the wall is completely homogeneous and if the load is not eccentric. The test was conducted

at 3 measurement points, two on the ground floor and one on the first floor. The results are shown in Table 2.



Figure 3. Masonry shear strength testing



Figure 4. The determination of the existing compressive stress in the masonry

Two flat jacks connected to a single hydraulic pump must be used in order to determine the stress-strain dependence of masonry. The test is performed in the same location where the vertical compressive stress test was performed, creating another hole above the existing one (used to determine vertical pressure), Figure 5. Flat jacks are inserted into parallel horizontal openings in the masonry and the compressive stress is applied by locally applying pressure to the jacks. Devices for measuring strain are placed in between flat jacks, and the stress and strain values are measured simultaneously, which enables the determination of the modulus of elasticity, Table 2.

Table 2. The results of mechanical properties of masonry

Position	Measurement point	Compressive stress $\sigma_0$ (MPa)	Modulus of elasticity (MPa)	Shear strength without compressive stress $f_{V0}$ (MPa)
Ground floor	FJ-PR-1	0,54	4020	0,171
Ground floor	FJ-PR-2	0,43	4122	0,825
First floor	FJ-1K-1	0,59	3407	0,134
<b>Average</b>			<b>3850</b>	<b>0,377</b>

The shear strength of masonry without compressive stress  $f_{V0}$  was also determined experimentally using flat jacks at 3 measuring points, Table 2. In this method the compressive stress  $\sigma_0$  in the masonry is checked during the shear test, Figure 6. During the test, the coefficient of friction  $\mu$  is also determined. The shear strength of the masonry without compressive stress  $f_{V0}$  can be expressed as follows:

$$f_{V0} = f_V - \mu \cdot \sigma_0 \quad (1)$$



Figure 5. Elasticity modulus test



Figure 6. The shear strength of masonry without compressive stress

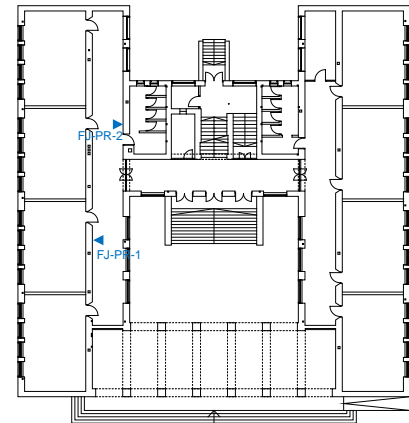


Figure 7. Measurement point locations on ground floor

## 2.2 Experimental research of dynamic properties

Within the experimental investigation of highschool in Sisak, operational modal analysis (OMA) was used to determine structural dynamic parameters. Unlike classical experimental modal analysis (EMA), the OMA method does not require known excitation. The experimental investigation was performed by using piezoelectric accelerometers (PCB Piezotronics, type 393B31 with nominal sensitivity of 10 V/g, PCB Piezotronics, Depew, NY, USA), an analyzer (Bruel and Kjaer, type 3560c, Bruel and Kjaer, Nærum, Denmark) and associated software. The measurement points were defined in 64 points, 32 in first floor and 32 in second floor, Figure 8. The measurement was performed at each of the measuring points in two perpendicular directions, x and y. Two reference accelerometers were placed in measuring point 213. Frequency domain decomposition (FDD) was used for the estimation of mode shapes. The values of experimentally obtained frequencies for the concerned mode shapes were read from the characteristic record, Figure 9. The results are shown in Table 3.

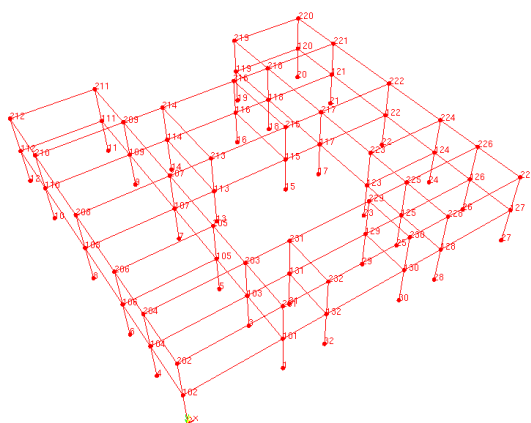


Figure 8. Dynamic properties measuring points in 3D

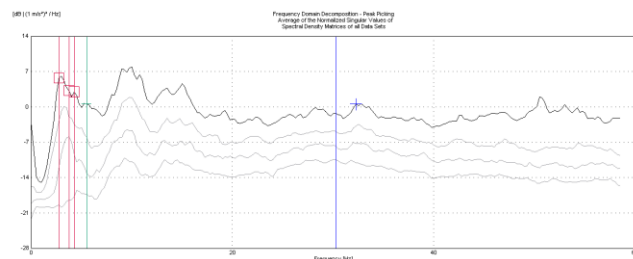


Figure 9. Characteristic record of frequency domain decomposition (FDD) for the determination of natural frequencies

Table 3. Values of first four experimentally obtained frequencies

Modal shape	Natural frequency [Hz]
1	2,98
2	3,96
3	4,45
4	5,92

### 3 Numerical analysis

The numerical model was developed in SCIA software. The material properties of the masonry used in the model are listed in Table 4. For data not obtained by experimental tests, the values according to EN 1996-1-1 [6] and EN 1998-1 [7] apply. For the modulus of elasticity, the average value of 3850 MPa obtained from three experimental tests, is used. The shear modulus  $G$  is calculated as follows:

$$G = 0.4 \cdot E \quad (2)$$

The characteristic compressive strength  $f_k$  can be calculated as

$$f_k = K \cdot f_b^{0,7} \cdot f_m^{0,3}, \quad (3)$$

where  $K$  is a constant assumed to be as  $K = 0.55$  according to [6],  $f_b$  is the compressive strength of the masonry unit, and  $f_m$  is the compressive strength of the masonry mortar. According to [8],  $f_b$  is assumed as 9.52 MPa, and according to [6],  $f_m = 1.0$  MPa. Characteristic flexural strengths of masonry  $f_{xk1}$  and  $f_{xk2}$  are determined according to [6].

Table 4. Mechanical properties of masonry in numerical model

Density (kg/m <sup>3</sup> )	1800
Modulus of elasticity $E$ (MPa)	3850
Shear modulus $G$ (MPa)	1540
Charasteristic compressive strength $f_k$ (MPa)	2.66
Charasteristic initial strength, under zero compressive stress $f_{vk0}$ (MPa)	0.377
Charasteristic flexural strength of masonry having the plane of failure parallel to the bed joints $f_{xk1}$ (MPa)	0.1
Charasteristic flexural strength of masonry having the plane of failure perpendicular to the bed joints $f_{xk2}$ (MPa)	0.2

The numerical model was created based on the defined geometry and the material properties determined by experimental tests. Walls and solid slabs were modeled with standard plane elements, rib-reinforced slabs were modeled with coupled plane elements, and beam-reinforced slabs are a plane element connected by means of rigid rods to a beam or rod element. For the boundary conditions, pinned bearings under the load-bearing walls of the basement and fixed bearings on the columns were assumed. The numerical model of the building is shown in Figure 10. The roof of the building was not modeled as part of the building structure, so a submodel of the roof was created to calculate the load transfer, Figure 11. The reactions from the dead weight of the roof were calculated and applied to the model. The weight of the roof is necessary to define the self-weight of the structure and to determine the dynamic parameters of the structure. For the calculation of the dynamic parameters, it is necessary to convert the input load into mass.

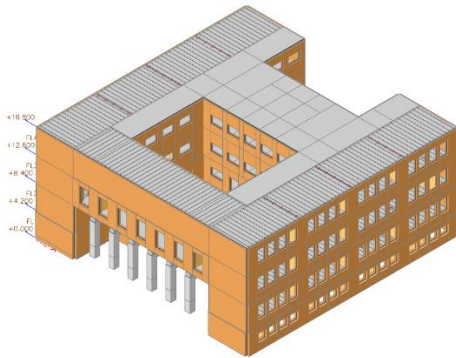


Figure 10. Numerical model of the building

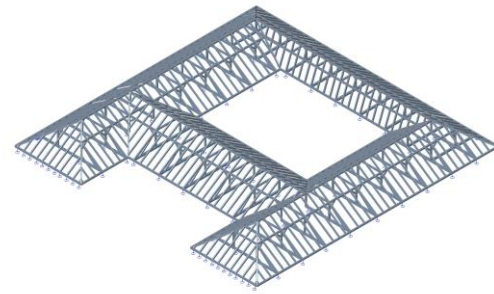


Figure 11. Submodel of the roof

The staircase was introduced into the model through the forces caused by the weight of the staircase at the point of support. For the calculation of the dynamic parameters it was necessary to convert the forces into mass, Figure 12. Partition walls are introduced into the model by the forces caused by the dead weight of the partition wall. In the numerical model, the forces are converted to mass to calculate the dynamic parameters. Since all partitions are damaged, they are defined as mass in the model, since it is assumed that they do not contribute to the stiffness, Figure 13.

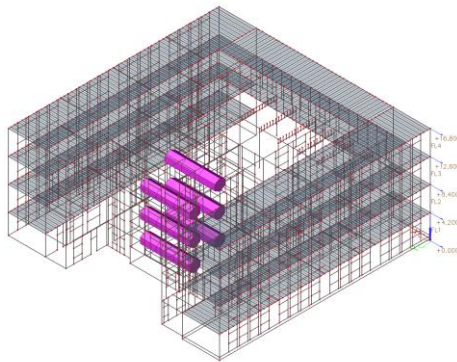


Figure 12. The mass of the staircase display

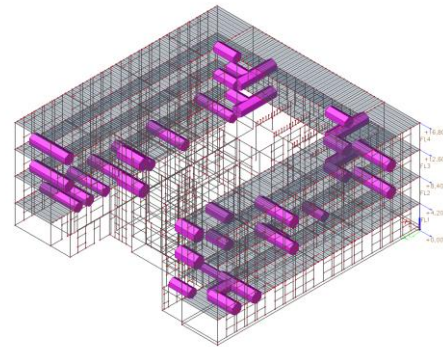


Figure 13. The mass of one part of the partition walls display

#### 4 Model calibration

In the numerical model of the structure, the vertical compressive stress caused by the dead weight was read at the measurement points where the compressive stress determination test was performed, Figure 14. A comparison of the existing compressive stress of the walls was performed, Table 5. The numerically determined stress results for the ground floor roughly correspond to the experimental results, but the stress read at the 1st floor differs significantly from the experimental result.

Table 5 Comparison of numerical and experimental results of compressive stress

Position	Measurement point	Experimental compressive stress $\sigma_0^{exp}$ (MPa)	Numerical compressive stress $\sigma_0^{num}$ (MPa)
Ground floor	FJ-PR-1	0,54	0,55
Ground floor	FJ-PR-2	0,43	0,35
First floor	FJ-K-1	0,59	0,38

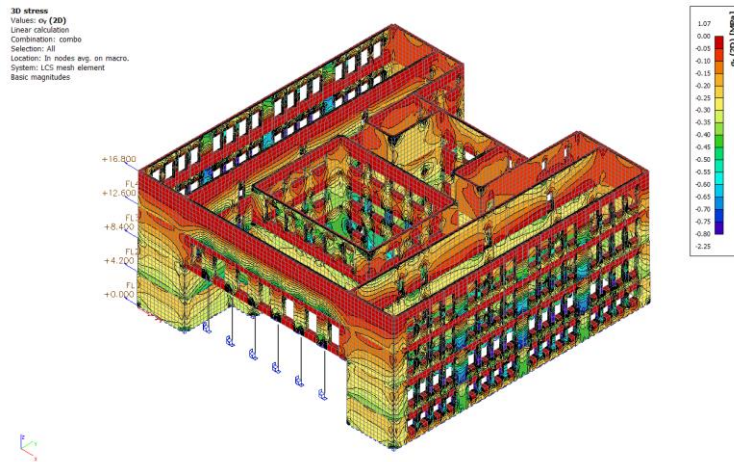


Figure 14. Compressive stress display in numerical model

The experimentally determined frequencies for the relevant mode shapes are compared with the numerically determined values. Although the numerically determined modal shapes agree with the experimental obtained shapes, a significant deviation of the frequency results can be seen in Table 6.

Table 6. Experimental and numerical frequencies comparison

Modal shape	$f^{exp}$ (Hz)	$f^{num}$ (Hz)	Deviation (%)
1	2,98	4,22	41,6
2	3,96	5,75	45,2
3	4,45	6,42	44,3
4	5,92	9,64	62,8

The results of the initial global numerical model agreed with the results of the local experimental tests, but the values of the frequencies of the numerical model compared with the experimental results were not satisfactory. Therefore, the improvement of the model in terms of the frequencies of the structure was approached through a whole series of iterations.

#### 4.1 First iteration - boundary condition

A comparison of frequencies was made with respect to the change in boundary conditions. The numerical model retained the entered mass of the self-weight of the structure and the mechanical properties of the material. The results for fixed boundary conditions and pinned boundary conditions under the load-bearing walls of the structure are shown graphically, Figure 15. The applied boundary conditions showed no significant effect on the results of the structure's frequency. Therefore, a pinned boundary condition was used in the further analysis.

#### 4.2 Second iteration - partitions

A comparison was also made of the frequency of numerical models in which the partitions were replaced with the appropriate mass, as described previously, and the model in which the partitions were modeled with a standard type of finite element of the wall surface, Figure 16. According to the standard [6], the characteristic flexural strengths of the masonry were entered. The modulus of elasticity, characteristic compressive strength and characteristic shear strength were taken from the tests described in section 2.1. In the numerical model, the mechanical properties of the solid brick wall material and the pinned boundary conditions were retained.

In the numerical model where the partitions were modeled as finite elements, the frequency of the structure increased compared to the numerical model where the partitions were input as mass. It can be concluded that the partitions contribute to the stiffness of the structure. However, in the following, the modeling of the partitions by mass in exchange for finite elements was retained in the numerical model because visual inspection revealed the damage of the partitions, then by inputting the seismic load to the numerical model, a significant excess of stress was found in the partitions, and insufficient thickness of each partition and excessive slenderness were found when the basic requirements were checked. Modeling of partitions using mass also contributes to a smaller number of finite elements.

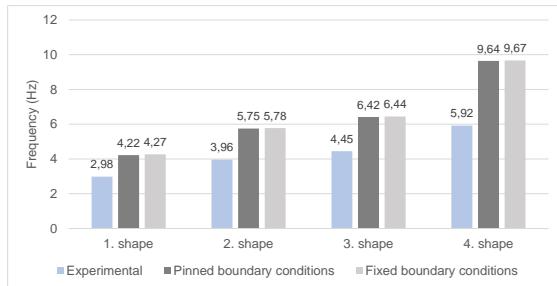


Figure 15. The frequencies for fixed boundary conditions and pinned boundary conditions

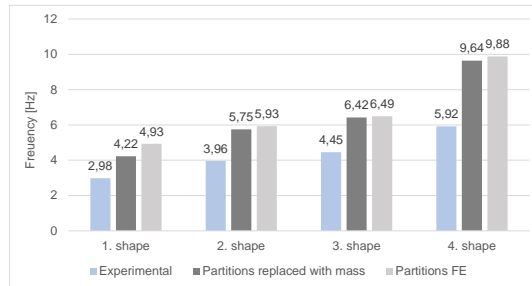


Figure 16. Frequency results depending on different partition modelling

### 4.3 Third iteration – damaged model

#### a) Reduction of the modulus of elasticity in damaged elements

The numerical analysis of the dynamic parameters is carried out by a linear analysis, which proves to be unsuitable for masonry because of its nonlinear behavior. Therefore, an attempt is made to describe the structure numerically, taking into account the existing damage. The damages are simulated on the numerical model by reducing the stiffness of the finite elements belonging to the damaged parts of the structure [4]. In order to reduce the difference between the experimentally and numerically determined dynamic parameters, a model is presented below in which an attempt is made to reduce the stiffness of the finite elements belonging to the damaged wall. The observed damage to the ground floor and the first floor structure is shown in Figure 17 and Figure 18. In the numerical model, the damaged parts of the structure are modeled with finite elements to which a material with modified properties, i.e. with reduced elastic modulus, is assigned. The reduction of the elastic modulus was performed in several steps, with the elastic modulus being reduced by 10% in each step. The numerical model retained the mechanical properties of the masonry, the pinned boundary conditions and the added masses of the non-structural elements. By reducing the elastic modulus, a reduction in the natural frequency of the damaged numerical model can be observed, Figure 19. Nevertheless, satisfactory results were not achieved by imitating the damaged parts of the structure using finite elements with a reduced elastic modulus.

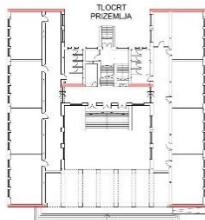


Figure 17. Damaged masonry in ground floor

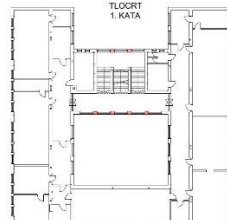


Figure 18. Damaged masonry in first floor

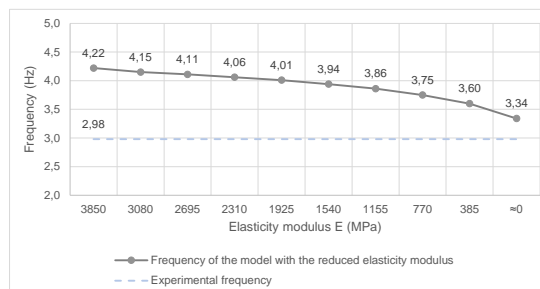


Figure 19. Frequency of the model with reduced elastic modulus of damaged elements, 1. modal shape



## b) Reduction of elastic modulus at diagonal crack location

Since satisfactory results were not obtained for the model with reduced elastic modulus in damaged elements of the building, a new approach for modeling damaged parts of the structure was introduced. According to the recommendations of [4], the numerical simulation of the crack pattern was performed by defining finite elements with a reduced elastic modulus  $E \approx 0$  MPa at the crack location, Figure 20. The elastic modulus is not zero, but was reduced to 100 MPa to avoid errors in the numerical calculation. The numerical model kept the mechanical properties of the masonry, set the pinned conditions and added the masses of the nonstructural elements. It can be seen that the frequency decreases with the introduction of the assumption of damaged finite elements. However, even with these models, the frequency is quite high compared to the experimental results, Table 7.

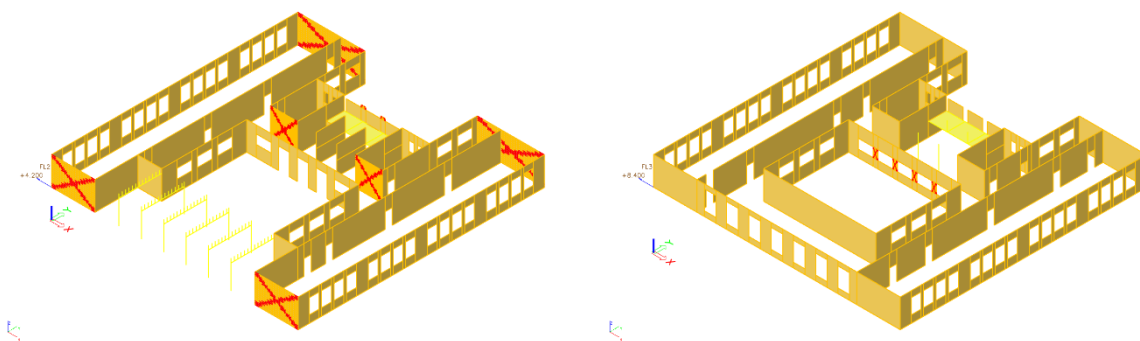


Figure 20. Numerical model with reduced elastic modulus at crack location in ground floor (left) and first floor (right)

Table 7. The comparison of experimental frequency and numerical frequency on model with diagonal damage

Modal shape	Frequency (Hz)		Difference (%)
	Experimental	Numerical	
1	2,98	3,78	26,8
2	3,96	5,29	33,6
3	4,45	6,29	41,3
4	5,92	9,43	59,3

### 4.4 Forth iteration - Reduction of the global elastic modulus

In the next iteration, the change in global elastic modulus was performed in increments of 500 MPa. Pinned boundary conditions were kept in the numerical model, the masses of non-structural elements were added, and the elastic modulus was reduced along the diagonal cracks of the damaged elements.

The obtained results of the frequency, depending on the reduction of the global elastic modulus, for the first modal shape are shown in the Figure 21. where the approaching of the results to the experimental values is visible. The modulus of elasticity at the level of 2000 MPa gives a very small deviation compared to the experimental result. The Table 8. shows a comparison of the experimental frequency and the frequency of the damaged numerical model with a global elastic modulus at the level of 2000 MPa. A small difference in natural frequency is observed for the first three modal shapes, while the frequency of the fourth modal shape has a larger deviation from the experimental result.

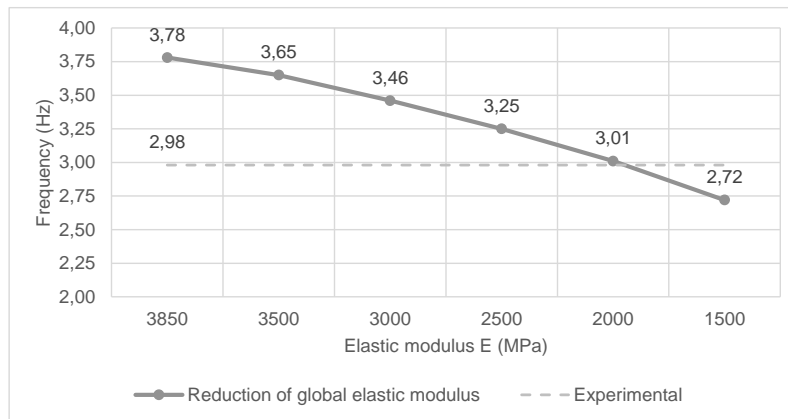


Figure 21. Results of the frequency, depending on the reduction of the global elastic modulus, for the 1. modal shape

Table 8. The comparison of experimental frequency and numerical frequency on model with a global elastic modulus reduced to 2000 MPa

Modal shape	Frequency (Hz)		Difference (%)
	Experimental	Numerical	
1	2,98	3,01	1,0
2	3,96	4,12	4,0
3	4,45	4,72	6,1
4	5,92	8,04	35,8

## 5 Discussion

The results of the natural frequencies of the initial numerical model compared to the experimental results were not satisfactory. Therefore, the model was updated through a whole series of iterations: modification of the boundary conditions, modelling of partition walls, modelling of the damage on structural elements and modification of the global stiffness of the structure, Figure 22. In relation to the initial numerical model, no significant differences in the frequencies of the structure were obtained by changing the boundary conditions of the numerical model. Then the comparison between the numerical model with the modelled partitions and the numerical model with the input mass of the partitions was started. The result was a higher frequency of the models with modelled partitions as the stiffness of the structure increased. In subsequent iterations, structural damage was added to the numerical model. The damage was first modelled by reducing the elastic modulus of the damaged parts of the building, but the results of the frequencies were not satisfactory. Then, damage modelling was started by reducing the elastic modulus of the finite elements along the cracks. In the end, the global stiffness was additionally reduced for this model by almost 50 % of the experimental values. Based on the mentioned assumptions introduced in the global numerical model, satisfactory results were obtained for the natural frequencies of the structure compared to the real behaviour of the structure.

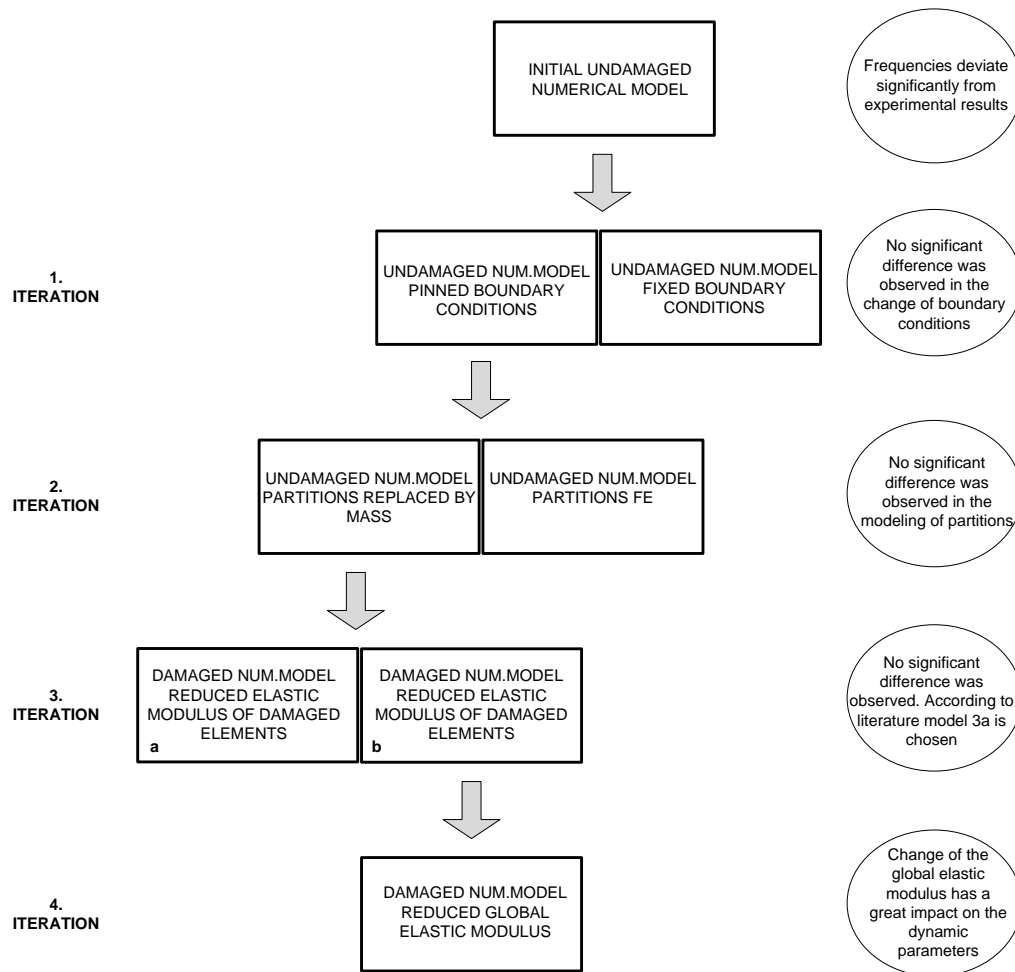


Figure 22. Flow chart of numerical model iteration

## 6 Conclusion

Experimental determination of mechanical properties of masonry and dynamic parameters of the structure can improve the accuracy of numerical models of structures. Determination of mechanical properties does not always give the correct results. In this case, the experimentally determined elastic modulus was reduced by almost 50% in the numerical model to obtain satisfactory results for the natural frequencies. The described uncertainty of the experimental results of the mechanical properties of the masonry can be eliminated by increasing the number of tests performed to obtain the global mechanical properties of the structure. However, such tests are time consuming and very expensive. Moreover, an attempt can be made to verify the assumptions of the performed tests of the mechanical properties of the masonry in order to make them more effective. Accordingly, the examination of the mechanical properties of the masonry could be directed to a more applicable and less expensive method, capable of determining the mechanical properties of the masonry at many more locations in the structure.

Apart from the reliability of the numerical model and the calibration of the numerical model analyzed here, by repeating the test after the future renovation under the condition of unchanged building mass, the experimentally determined dynamic parameters of the structure can be used to verify the effects of the future renovation of the building.

## References

- [1] J. Krolo, D. Damjanović, I. Duvnjak, M. Frančić Smrkić, M. Bartolac, and J. Koščak, “Methods for determining mechanical properties of walls,” *Gradjevinar*, vol. 73, no. 2, pp. 127–140, 2021, doi: 10.14256/JCE.3063.2020.
- [2] S. Ereiz, I. Duvnjak, D. Damjanović, and M. Bartolac, “Analysis of seismic action on the tie rod system in historic buildings using finite element model updating,” *Buildings*, vol. 11, no. 10, 2021, doi: 10.3390/buildings11100453.
- [3] L. F. Ramos, L. Marques, P. B. Lourenço, G. De Roeck, A. Campos-Costa, and J. Roque, “Monitoring historical masonry structures with operational modal analysis: Two case studies,” *Mech. Syst. Signal Process.*, vol. 24, no. 5, pp. 1291–1305, 2010, doi: 10.1016/j.ymssp.2010.01.011.
- [4] D. Pellegrini *et al.*, “Modal analysis of historical masonry structures: Linear perturbation and software benchmarking,” *Constr. Build. Mater.*, vol. 189, pp. 1232–1250, 2018, doi: 10.1016/j.conbuildmat.2018.09.034.
- [5] Lulić, Luka; Stepinac, Mislav; Damjanović, Domagoj; Duvnjak, Ivan; Bartolac, Marko; Hafner, “The role of flat-jack testing after recent earthquakes,” in *Proceedings of the 3rd European Conference on Earthquake Engineering & Seismology*, 2022, pp. 289–296.
- [6] *EN 1996-1-1 Eurocode 6 - Design of masonry structures - Part 1-1: General rules for reinforced and unreinforced masonry structures*. 2011.
- [7] *EN 1998 -1 Eurocode 8 - Design of structures for earthquake resistance - Part 1 : General rules, seismic actions and rules for buildings*. 2011.
- [8] M. Uroš, M. Todorčić, M. Crnogorac, J. Atalić, M. Šavor Novak, and S. Lakušić, *Potresno inženjerstvo - Obnova zidanih zgrada*.